Feature Article

Assembly of the Transition Metal Substituted Polyoxometalates $ZnW_{11}M(H_2O)O_{39}^{n-}$ (M = Mn, Cu, Fe, Co, Cr, Ni, Zn) on 4-Aminobenzoic Acid Modified Glassy Carbon Electrode and Their Electrochemical Study

Jianyun Liu, Long Cheng, and *Shaojun Dong**

Laboratory of Electroanalytical Chemistry, Changchun Institute of Applied Chemistry, Chinese Academy of Sciences, Changchun 130022, P. R. China; e-mail: dongsj@ns.ciac.jl.cn

Abstract

Through layer-by-layer assembly, a series of undecatungstozincates monosubstituted by first-row transition metals, $ZnW_{11}M(H_2O)O_{39}^{n-}$ (M = Cr, Mn, Fe, Co, Ni, Cu or Zn) were first successfully immobilized on a 4-aminobenzoic acid modified glassy carbon electrode surface. The electrochemical behaviors of these polyoxometalates were investigated. They exhibit some special properties in the films different from those in homogeneous aqueous solution. The Cu-centered reaction mechanism in the $ZnW_{11}Cu$ multilayer film was described. The electrocatalytic behaviors of these multilayer film electrodes to the reduction of H_2O_2 and BrO_3^- were comparatively studied.

Keywords: Polyoxometalates, 4-Aminobenzoic acid modified electrode, Layer-by-layer assembly, Electrochemical behavior, Electrocatalytic reduction of H_2O_2 and BrO_3^-

1. Introduction

The transition-metal-substituted polyoxometalates (TMSPs) have attracted much attention and interest because of their catalytic reactivity similar to metalloporphyrin [1, 4]. Various TMSPs have been prepared and their electrochemical and catalytic properties studied [3–13]. Most of these studies focused mainly on the electrochemistry in homogeneous aqueous solution. Rong et al. found that some transition metal-substituted heteropolytungstate anions adsorbed on mercury electrode surface but not on the glassy carbon electrode surface [14, 15]. Fe-substituted heteropolytungstate anions were entrapped in the polymer film, but the stability was poor [16–18]. So it is necessary to explore a new method for immobilizing TMSPs on an electrode surface.

It is feasible to fabricate polyoxometalate-containing multilayer films, such as SiW_{12}, P_2Mo_{18} and PMo_{12} [19–26]. It have been proven that by layer-by-layer assembly method, the resulting multilayer films are attractive for sensing and electronic device because of the thickness controllability, composite adjustability, film uniformity and stability, compared with the traditional methods such as adsorption, entrapped in polymer and electrodeposition [23–26]. In this article, a series of TMSPs, $ZnW_{11}M(H_2O)O_{39}^{n-}$ (M = Cr, Mn, Fe, Co, Ni, Cu or Zn) (abbreviated as $ZnW_{11}M$) were successfully immobilized on a 4-aminobenzoic acid modified glassy carbon electrode (GCE) through layer-by-layer assembly with a quaternized poly(4-vinylpyridine) partially complexed with $[Os(bpy)_2Cl]^{1+/2+}$ (QPVP-Os) as counterions. The electrochemical behaviors of the multilayer film were investigated systematically by cyclic voltammetry, which is a little different from those in homogeneous aqueous solution [27]. The electrocatalytic properties of these $ZnW_{11}M$ multilayers for the reduction of H_2O_2 and BrO_3^- were comparatively studied for the first time.

2. Experimental

2.1. Reagents and Instrumentation

The potassium salts of this TMSP series, $K_nH[ZnW_{11}M(H_2O)O_{39}] \cdot H_2O$ (M = Cr, Mn, Fe, Co, Ni, Cu, Zn) and polycation, QPVP-Os were prepared according to the literature [28] and [29], respectively. Solutions of 4-aminobenzoic acid (4-ABA), H_2O_2 and $NaBrO_3$ were freshly prepared before use. Other chemicals were of reagent grade and used as received. Water was purified using Millipore Milli-Q water purification system. Buffer solutions were prepared from 0.2 M $Na_2SO_4 + H_2SO_4$ (pH < 3) and 0.2 M $NaAc + HAc$ (pH 3–6).

Electrochemical experiments were performed with CHI 660 voltammetric analyzer (USA) in a conventional three-electrode cell whose configuration was the same as that in the previous articles [24, 25]. Solutions were deaerated for at least 20 min with high-purity N_2 and kept under a pressure of this gas during the experiments.

2.2. Fabrication of ZnW₁₁M-Containing Multilayer Films

Modification of 4-ABA on GCE was performed according to those described [24, 25]. The GCE surface grafted with 4-ABA possesses a carboxyl-terminated monolayer, which can adsorb the oppositely charged polyions. The 4-ABA/GCE was first placed in 0.5 mg/mL QPVP-Os + NaAc buffer (pH 3.8) and then scanned between 0.6 and 0 V at a scan rate of 100 mV s⁻¹ for 25 cycles. After that, the electrode was transferred to 0.1 M ZnW₁₁M + NaAc buffer (pH 3.8) resulting in one layer of ZnW₁₁M by scanning between 0.6 and −0.4 V similar to those described above. When the resulting electrode was placed alternately in QPVP-Os and ZnW₁₁M solutions, the ZnW₁₁M multilayers were formed. The cyclic potential sweeps for 25 cycles proved to be sufficient since the peak currents of ZnW₁₁M did not increase when scanning for more cycles.

3. Results and Discussion

3.1. Electrochemical Behavior of ZnW₁₁M Multilayer Film Immobilized on 4-ABA-Modified GCE

Through the attachment of 4-ABA to the GCE, the modified electrode 4-ABA/GCE was negatively charged at higher pH (pH > $pK_a = 3.1$) [24]. QPVP-Os was first deposited on the modified GCE through electrostatic interaction. Figure 1A shows the Os-centered redox reaction of the QPVP-Os monolayer adsorbed on 4-ABA/GCE (solid line). Compared with the CV curve of 4-ABA-modified electrode (dotted line), one pair of anodic / cathodic peaks appear and its formal potential (E_f), taken by the average value of the anodic and cathodic peak potentials, was 0.32 V, which was related to the Os³⁺/²⁺ redox couple in the polycations. Cyclic voltammograms (CVs) of the QPVP-Os monolayer at different scan rates (Fig. 1B) indicate that the peak currents are proportional to scan rates (inset of Fig. 1B). Inset presents the linear relationship between the cathodic peak current and the scan rates. Moreover, the formal potential is independent of scan rate, and the cathodic peak current is almost the same as that of anodic one. These suggest that the electron-transfer is a reversible surface process [30].

Based on the description in experimental section, the ZnW₁₁M multilayer films were successfully fabricated by layer-by-layer assembly on QPVP−Os/4-ABA/GCE. Figure 2 shows the CVs of three representative ZnW₁₁M (M = Mn (A), Cu (B), Co (C)) and the saturated parent heteropolyanion ZnW₁₂ (D) multilayer films. Clearly, in the negative potential range between −0.2 V and −0.85 V the redox waves from W-O framework increase uniformly with the growth of the multilayer films. Insets of Figure 2 show the linear relationship between the corresponding redox currents of polyoxometalates and their layer numbers. And the similar redox waves appear at about 0.25 V in Figure 2 (A, C, D), which derive from the Os-centered redox reaction of QPVP-Os polycation. In ZnW₁₁Cu-containing
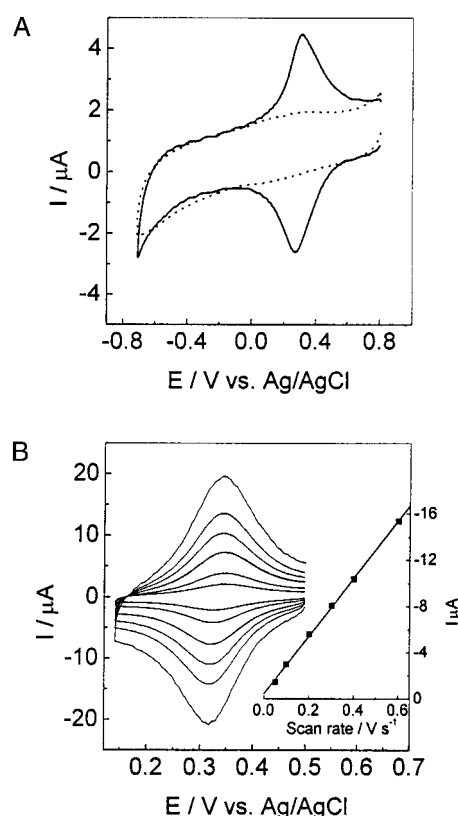
Fig. 1. A) CVs of QPVP-Os/4-ABA/GCE (solid line) and 4-ABA/GCE (dotted line) in pH 3.8 acetate solution. B) CVs of QPVP-Os monolayer at QPVP-Os/4-ABA/GCE in pH 3.8 acetate buffer at different scan rates. From inside to outside: 20, 50, 100, 200, 300, 400, 500 and 600 mV s⁻¹, respectively.

multilayers, the Os-centered waves are masked by the Cu redox wave of ZnW₁₁Cu and not seen separately. ZnW₁₁Cr, ZnW₁₁Ni and ZnW₁₁Zn multilayers exhibit the similar voltammograms to that of ZnW₁₁Co, and are not shown here.

The electron numbers participating in the redox reactions of W−O framework were estimated from the peak potential full-width at half-maxium of peak current, E_{fwhm}, being marked in the corresponding CV curves. Taking the two-electron reactions as examples, these E_{fwhm} values are larger than the theoretical predicted value (90/n) of 45 mV for an ideal two-electron surface wave [30]. Compared with the electrochemical behavior of ZnW₁₁M in homogeneous aqueous solutions [27], the electron numbers participating in the redox reaction of the W−O framework in the multilayer film are similar, but ZnW₁₁M multilayers on the 4-ABA/GCE show some different electrochemical behaviors (Fig. 2). First, the W-centered one-electron peaks, appearing at about −0.4 V in ZnW₁₁M homogeneous solutions [27], are hardly discerned on the ZnW₁₁M multilayer films; and the third two-electron peaks are not shown because of the overlap with the reaction of hydrogen evolution [31–33]. Second, the oxidation waves (peak I′₂ₑ, II′₂ₑ in Fig. 2A, 2B and 2C) corresponding to two-electron reduction of W−O frameworks distort with the growth of the
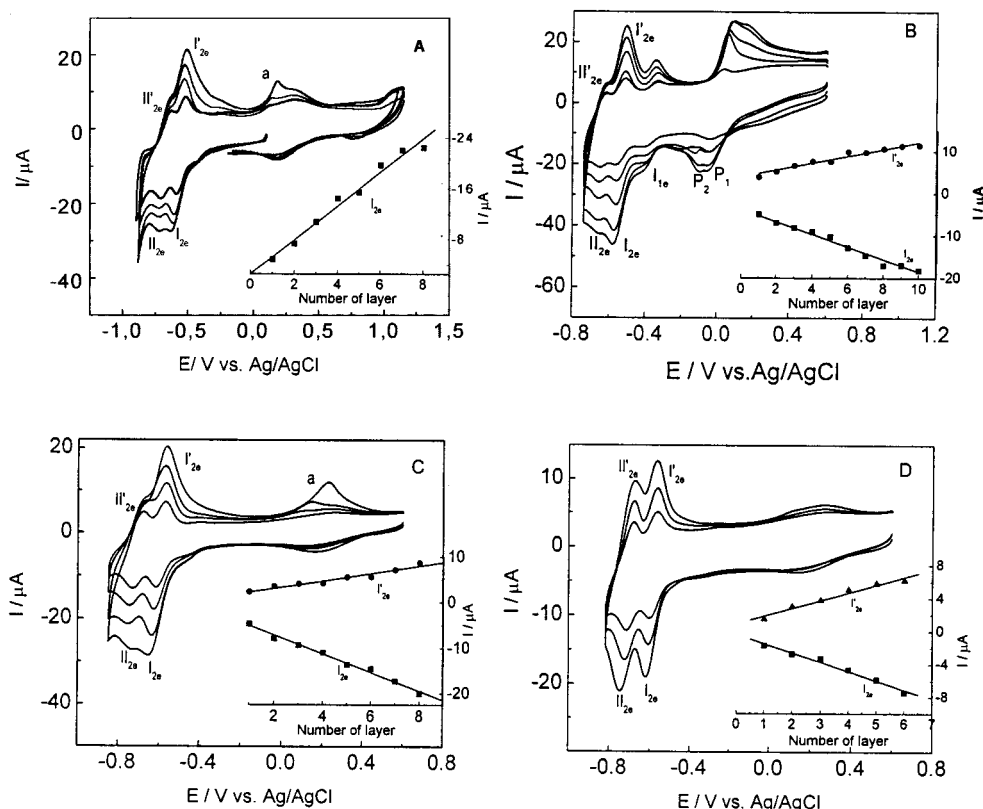
Fig. 2.   CVs of ZnW$_{11}$M multilayers on 4-ABA-modified GCE in pH 3.8 acetate buffer. Scan rate: 100 mV s^{-1}. A) 2, 4, 6 and 8 layers of ZnW$_{11}$Mn, B) 2, 4, 6, 8 and 10 layers of ZnW$_{11}$Cu, C) 2, 4, 6 and 8 layers of ZnW$_{11}$Co, and D) 2, 4 and 6 layers of ZnW$_{12}$.

films, whereas the redox peak of the parent heteropolyanion ZnW$_{12}$ multilayer film (Fig. 2D) shows a well-defined redox behavior. It indicates that the substituted metals have a certain influence on the electron-transfer when the film becomes thicker. Third, when the TMSPs film grows above 4-layer thick, a small shoulder peak (wave a of Fig. 2A and C) accompanied with the oxidation of QPVP–Os always appears at about +0.2 V, and enhances with the growth of the multilayer films. But it only emerges upon the appearance of tungsten reduction by carefully choosing the reversal potential in cyclic voltammetry, and increases with the negative shift of the reversal potential. Therefore, the unusual peak is relevant to the tungsten reduction product. However, no shoulder peak appears in CVs of the parent ZnW$_{12}$ multilayer film (Fig. 2D). We further fabricated the ZnW$_{11}$M multilayers with poly(diallyldimethylammonium chloride) as the counterions, and no shoulder peak was observed in CVs, either. It is supposed that there are some special interactions between the substituted transition metal atoms of ZnW$_{11}$M and QPVP-Os or between the lacunary anion ZnW$_{11}$ and Os from QPVP-Os in the film, though the reason is unclear up to now.

Substituted metal Mn in ZnW$_{11}$Mn multilayers (Fig. 2A) shows the electrochemical activity at about +1.1 V just like that in aqueous solution [27], though the growth of Mn-centered redox currents is irregular. However, Cu in ZnW$_{11}$ Cu multilayers shows different electrochemical behavior at

about −0.15 V from that in aqueous solution [27]. The CVs of 4 layers of ZnW$_{11}$Cu multilayers were conducted with different negative potential limits (Fig. 3). It is worth noting that two overlapped reduction peaks (P$_1$, P$_2$) are observed at −0.05 and −0.16 V, respectively, which are similar to the two one-electron reduction waves of Cu^{II} ions owing to the stabilization of Cu^I by the formation of benzotriazolate-Cu^I [34] and Cu^{I}Cl$_2^-$ [35, 36]. Keita et al. [10] also found the stepwise reduction of copper in Cu(II)-substituted P$_2$Mo$_2$
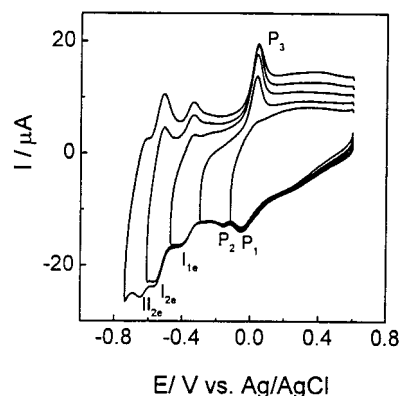
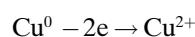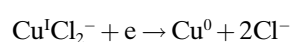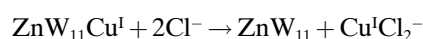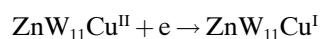Fig. 3.   CVs of 4 layers ZnW$_{11}$Cu on 4-ABA-modified GCE in pH 3.8 acetate buffer with different negative potential limits. Scan rate: 100 mV s^{-1}.

$W_{15}O_{61}$ complex aqueous solution but gave no detailed explanation. Free chloride ions in QPVP-Os polymer are entrapped partially in the multilayer films when constructing multilayers. It is reasonable to expect that the formation of $Cu^{I}Cl_2^-$ complex stabilizes Cu^I, then its further reduction will be retarded and two one-electron waves are observed. However, a single two-electron Cu^{II} reduction wave was observed in homogeneous solution [27]. Further, no stripping peaks appear if the reversal potential is not sufficiently negative to the appearance of the reduction peak P_2. So the sharp stripping peak (P_3) corresponds to an anodic stripping process of Cu^0 to Cu^{II} [27,37]. By comparison, the Cu-centered reactions in the multilayer films occur in terms of the mechanism [27, 35, 36].

$$ZnW_{11}Cu^{II} + e \rightarrow ZnW_{11}Cu^I$$

$$ZnW_{11}Cu^I + 2Cl^- \rightarrow ZnW_{11} + Cu^{I}Cl_2^-$$

$$Cu^{I}Cl_2^- + e \rightarrow Cu^0 + 2Cl^-$$

$$Cu^0 - 2e \rightarrow Cu^{2+}$$

$$ZnW_{11} + Cu^{2+} \rightarrow ZnW_{11}Cu^{II}$$
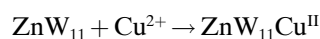
(All these processes happen in the multilayer films)

3.2. Electrocatalytic Properties of TMSPs Multilayer Film to BrO_3^- and H_2O_2

Usually, the active sites in TMSPs for the catalytic reaction are the transition metals. Figure 4A and 4B show the CVs of 6 layers $ZnW_{11}Mn$ and $ZnW_{11}Cu$ immobilized on 4-ABA/GCE in pH 1.2 solution containing various concentrations of BrO_3^-, respectively. As shown in Figure 4A, with the addition of BrO_3^-, the one-electron redox wave at -0.26 V becomes more and more distinct. Obviously, the catalytic reduction of BrO_3^- starts from the first W-centered one-electron redox waves, though this wave is unclear in electrolyte solution in the absence of BrO_3^- (dotted line in Fig. 4A). Inset shows the linear relationship between the catalytic currents and BrO_3^- concentration. $ZnW_{11}Cu$ multilayers have similar catalytic behavior to that of $ZnW_{11}Mn$ multilayers. Actually, the catalytic reduction of BrO_3^- starts at the Cu-centered reaction potential in $ZnW_{11}Cu$ film (Fig. 4B). The CVs of $ZnW_{11}Ni$ multilayers in various BrO_3^- concentrations were given here (Fig. 4C) for comparison.

The electrocatalytic properties of this series of $ZnW_{11}M$ on 4 layers of the multilayer electrode were further comparatively investigated and the results were listed in the Table 1. Clearly, both $ZnW_{11}Mn$ and $ZnW_{11}Cu$ multilayers catalyze the reduction of BrO_3^- and H_2O_2 with low overpotential. They have higher catalytic activity than the others. $ZnW_{11}Co$ and $ZnW_{11}Ni$ multilayers catalyze the reduction of BrO_3^- and H_2O_2 with large overpotential. While other $ZnW_{11}M$ multilayers have poor catalytic activity, similar to the parent ZnW_{12} multilayer film. Further, the
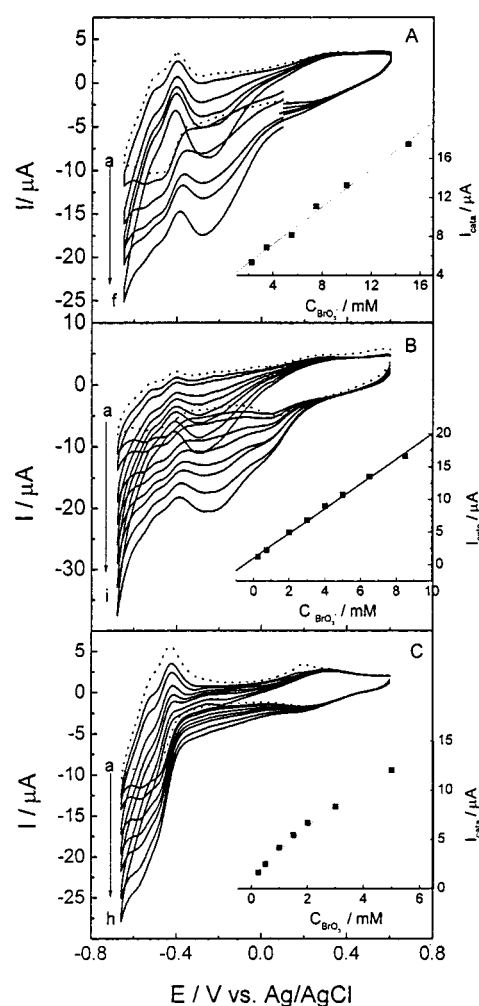
Fig. 4. CVs of 6 layers A) $ZnW_{11}Mn$, B) $ZnW_{11}Cu$ and C) ZnW_{11}Ni on 4-ABA-modified GCE in Na_2SO_4 (pH 1.2) solution containing different concentrations of BrO_3^-. A) a) – f) 0, 0.2, 3.5, 7.5, 10.0 and 15.0 mM BrO_3^-, respectively; B) a) – i) 0, 0.25, 0.75, 2.0, 3.0, 4.0, 5.0, 6.5 and 8.5 mM BrO_3^-, respectively; C) a) – h) 0, 0.25, 0.5, 1.0, 1.5, 2.0, 3.0, and 5.0 mM BrO_3^-, respectively.

catalytic current on 4 layers of multilayer film is not as great as that on the electrode with 6 layers of multilayer film (Fig. 4). Clearly, with increasing the layer number of ZnW_{11}M, the catalytic current enhances. This catalytic property of the multilayer film has been verified in many places [21, 25, 26].

The series of TMSPs have the same structure (Keggin-type), the same central heteroatom (Zn) and the same addendum (W). Therefore, the lacunary transition metals, especially the metals with redox activity, may have great effects on the electrochemical and electrocatalytic behavior of the polyoxometalates.

3.3. Stability of the TMSPs Multilayer Film

These three-dimensional TMSPs multilayer films were very stable except for $ZnW_{11}Fe$. Potential scanning in the range

Table 1. Comparison of the catalysis to the reduction of BrO_3^- and H_2O_2 on 4-ABA/GCE with 4 layers of TMSPs multilayer film.

TMSPs		$ZnW_{11}Mn$	$ZnW_{11}Cu$	$ZnW_{11}Fe$	$ZnW_{11}Co$	$ZnW_{11}Ni$	$ZnW_{11}Cr$	$ZnW_{11}Zn$	ZnW_{12}	bare GCE
BrO_3^- [c]	I_{cata} [a] (μA)	4.13	8.72	–	12.26	12.58	4.6	5.9	4.11	0
	E_{cata} [b] (V)	− 0.29	− 0.23	–	− 0.48	− 0.48	− 0.49	− 0.48	− 0.47	− 0.48
H_2O_2 [d]	I_{cata} [a] (μA)	10.47	11.80	–	19.20	3.00	2.5	1.3	3.82	0.4
	E_{cata} [b] (V)	− 0.30	− 0.20	–	− 0.70	− 0.70	− 0.70	− 0.70	− 0.70	− 0.7

[a] I_{cata} was obtained by subtracting the current in background solution from the reaction current at E_{cata}.
[b] E_{cata} represents the potential at which the catalytic current increases markedly.
[c] c (BrO_3^-) = 5 mM, supporting electrolyte: 0.2 M Na_2SO_4 (pH 1.2).
[d] c (H_2O_2) = 8 mM, supporting electrolyte: 0.2 M NaAc (pH 5.3). The results were the average values from three repeated experiments.
– Because of the instability of the $ZnW_{11}Fe$ film, the catalytic currents are not shown here.

from 0.6 to − 0.8 V in HAc buffer for 50 cycles at 200 mV s^{-1}, W-centered redox currents decreased only 6.5%. There was no great change when continuous scanning again. However, W-centered redox behavior of $ZnW_{11}Fe$ films was ill-defined, which is the same as that of $ZnW_{11}Fe$ homogeneous solution [27]. When the $ZnW_{11}Mn$ multilayers electrode were scanned continuously between − 1.0 V and + 1.15 V, Mn-centered redox waves diminished gradually, while the redox waves of W−O framework were almost unchanged. It is possible that some metal centers separate from their original co-ordinated state. Continuous potential scans of $ZnW_{11}Cu$ film between − 1.0 and 0.6 V did not reduce the Cu-centered redox current. But Cu redox wave diminished gradually in $ZnW_{11}Cu$ aqueous solution [27]. So the multilayer film can keep substituent Cu from losing. Work is in progress to find a more suitable strategy to keep the substituent metal Mn, Fe stable in their original state.

4. Conclusions

Usually, TMSPs are difficult to be immobilized on a carbon electrode surface. In this article, through grafting of 4-aminobenzoic acid on GCE, a series of undecatungstozincates monosubstituted by first-row transition metals, ZnW_{11} M (M = Cr, Mn, Fe, Co, Ni, Cu or Zn) multilayer films have been successfully fabricated on the modified GCE by layer-by-layer assembly with the polycation QPVP-Os as the counterion. Cyclic voltammetry proves the uniform growth of these TMSPs multilayers. Their electrochemical behaviors on the multilayer-modified electrode were discussed, which are different from those in homogeneous aqueous solution. These $ZnW_{11}M$ multilayers can catalyze the reduction of BrO_3^- and H_2O_2. By comparison, it has been found that the lacunary transition metals in $ZnW_{11}M$ multilayer films, especially those with electrochemical activity, have great effects on the electrochemical and electrocatalytic behavior of the heteropolyanions. The layer-by-layer assembly way for the multilayer fabrication has many advantages, such as thickness controllability, composite adjustability and film uniformity. And the carbon electrode is selected as a support substrate by reason that it

has good conductivity, resistance to environmental and chemical attack and a wide potential window in electrochemistry. These characteristics might lead to the potential applications of TMSPs multilayer films in the fields of sensors and microelectronic devices.

5. Acknowledgement

6. References

[1] M. T. Pope, *Heteropoly and Isopoly Oxometalates*, Springer-Verlag, New York **1983.**
[2] J. E. Toth, F. C. Anson, *J. Am. Chem. Soc.* **1989**, *111*, 2444.
[3] J. E. Toth, J. D. Melton, D. Cabelli, B. H. J. Bielski, F. C. Anson, *Inorg. Chem.* **1990**, *29*, 1952.
[4] C. Rong, F. C. Anson, *Inorg. Chem.* **1994**, *33*, 1064.
[5] J. C. Bart, F. C. Anson, *J. Electroanal.Chem. Interfacial Electrochem.* **1995**, *390*, 11.
[6] C. L. Hill, R. B. Brown, Jr., *J. Am. Chem. Soc.* **1986**, *108*, 536.
[7] S. Dong, X. Xi, M. Tian, *J. Electroanal. Chem.* **1995**, *385*, 227.
[8] B. Fabre, G. Bidan, *J. Chem. Soc., Faraday Trans.* **1997**, *93*, 591.
[9] T. McCormac, B. Fabre, G. Bidan, *J. Electroanal. Chem.* **1997**, *427*, 155.
[10] B. Keita, Y. W. Lu, L. Nadjo, R. Content, M. Abbessi, J. Canny, M. Richet, *J. Electroanal. Chem.* **1999**, *477*, 146.
[11] B. Keita, A. Belhouari, L. Nadjo, R. Content, *J. Electroanal. Chem.* **1998**, *442*, 49.
[12] B. Keita, F.Girard, L. Nadjo, R. Content, J. Canny, M. Richet, *J. Electroanal. Chem.* **1999**, *478*, 76.
[13] A. Müller, L. Dloczik, E. Diemann, M. T. Pope, *Inorg. Chim. Acta* **1997**, *257*, 231.
[14] C. Rong, F. C. Anson, *Anal. Chem.* **1994**, *66*, 3124.
[15] C. Rong, F. C. Anson, *Inorg. Chim. Acta* **1996**, *242*, 11.
[16] B. Fabre, G. Bidan, M. Laplowski, *J. Chem. Soc., Chem. Commun.* **1994**, 1509.
[17] K. K. Shiu, F. C. Anson, *J. Electroanal. Chem.* **1991**, *309*, 115.
[18] S. Gaspar, L. Muresan, A. Prtrut, I.C. Popescu, *Anal. Chim. Acta* **1999**, *385*, 111.
[19] C. Sun, J. Zhao, H. Xu, Y. Sun, X, Zhang, J. Shen, *J. Electroanal. Chem.* **1997**, *435*, 63.

[20] A. Kuhn, F.C, Anson, *Langmuir* **1996**, *12*, 5481.
[21] D. Martel, A. Kuhn, *Electrochim. Acta* **2000**, *45*, 1829.
[22] D. Ingersoll, P. J. Kulesza, L. R. Faulkner, *J. Electrochem. Soc.* **1994**, *141*, 140.
[23] L. Cheng, L. Niu, J. Gong, S. Dong, *Chem. Mater.* **1999**, *11*, 1465.
[24] J. Liu, L. Cheng, B. Liu, S. Dong, *Langmuir* **2000**, *16*, 7471.
[25] L. Cheng, J. Liu, S. Dong, *Anal. Chim. Acta* **2000**, *417*, 133.
[26] L. Cheng. S. Dong, *J. Electrochem. Soc.* **2000**, *147*, 606.
[27] L. Cheng, H. Sun, B. Liu, J. Liu, S. Dong, *J. Chem. Soc., Dalton Trans.* **1999**, *15*, 2619.
[28] J. Liu, Y. Wang, Q. Yang, Y. Chen, M. Li, C. Liu, S. Yang, *Polyhedron* **1996**, *15*, 717.
[29] A. P. Doherty, R. J. Forster, M. R. Smyth, J. G. Vos, *Anal. Chim. Acta* **1991**, *255*, 43.

[30] R. W. Murray, *Electroanalytical Chemistry*, Vol. 13 (Ed: A. J. Bard), Marcel Dekker, New York **1984**, pp 191–368.
[31] K. K. Kasem, F. A. Schultz, *Can. J. Chem.* **1995**, *73*, 858.
[32] G. Bidan, E. M. Genies, M. Lapkowski, *J. Chem. Soc., Chem. Commun.* **1999**, 533.
[33] B. Keita, D. Bouaziz, L. Nadjo, *J. Electroanal. Chem.* **1988**, *255*, 303.
[34] V. B. Nascimento, I.G.R. Gutz, *Electrochim. Acta* **1998**, *43*, 3423.
[35] S. Daniele, M. J. Pena, *Electrochim. Acta* **1993**, *38*, 165.
[36] G. Gunawardena, G. Hills, I. Montenegro, *J. Electroanal. Chem.* **1985**, *184*, 357.
[37] M. A. Baldo, C. Bragato, G. A. Mazzocchin, S. Daniele, *Electrochim. Acta* **1998**, *43*, 3413.